Neuron
Article

The Cerebrospinal Fluid Provides a Proliferative Niche for Neural Progenitor Cells

Maria K. Lehtinen,[1,2,9] Mauro W. Zappaterra,[1,2,3,9] Xi Chen,[1,2,4] Yawei J. Yang,[1,2,3,4] Anthony D. Hill,[1,2] Melody Lun,[1,2,6] Thomas Maynard,[5] Dilenny Gonzalez,[1,2] Seonhee Kim,[8] Ping Ye,[7] A. Joseph D'Ercole,[7] Eric T. Wong,[6] Anthony S. LaMantia,[5] and Christopher A. Walsh[1,2,3,*]

[1]Division of Genetics, Howard Hughes Medical Institute, and Manton Center for Orphan Disease Research, Children's Hospital Boston, Boston, MA 02115, USA
[2]Broad Institute of MIT and Harvard, Cambridge, MA 02142, USA
[3]Program in Biological and Biomedical Sciences, Harvard Medical School, Boston, MA 02115, USA
[4]Harvard-MIT Division of Health Sciences and Technology, Harvard Medical School, Boston, MA 02115, USA
[5]Department of Pharmacology and Physiology, The George Washington Institute for Neuroscience, The George Washington University School of Medicine, Washington, DC 20037, USA
[6]Brain Tumor Center & Neuro-Oncology Unit, and Division of Signal Transduction, Beth Israel Deaconess Medical Center, Boston, MA 02215, USA
[7]Department of Pediatrics, The University of North Carolina at Chapel Hill, Chapel Hill, NC 27599, USA
[8]Pediatric Research Center, Department of Pediatrics, University of Texas Health Science Center at Houston, MSE411, 6431 Fannin Street, Houston, TX 77030, USA
[9]These authors contributed equally to this work
*Correspondence: christopher.walsh@childrens.harvard.edu
DOI 10.1016/j.neuron.2011.01.023

SUMMARY

Cortical development depends on the active integration of cell-autonomous and extrinsic cues, but the coordination of these processes is poorly understood. Here, we show that the apical complex protein Pals1 and Pten have opposing roles in localizing the Igf1R to the apical, ventricular domain of cerebral cortical progenitor cells. We found that the cerebrospinal fluid (CSF), which contacts this apical domain, has an age-dependent effect on proliferation, much of which is attributable to Igf2, but that CSF contains other signaling activities as well. CSF samples from patients with glioblastoma multiforme show elevated Igf2 and stimulate stem cell proliferation in an Igf2-dependent manner. Together, our findings demonstrate that the apical complex couples intrinsic and extrinsic signaling, enabling progenitors to sense and respond appropriately to diffusible CSF-borne signals distributed widely throughout the brain. The temporal control of CSF composition may have critical relevance to normal development and neuropathological conditions.

INTRODUCTION

Neural development involves a dynamic interplay between cell autonomous and diffusible extracellular signals that regulate symmetric and asymmetric division of progenitor cells (Johansson et al., 2010). In mammalian neural progenitors, homologs of *C. elegans* and *Drosophila* polarity proteins, including Par3 (partitioning defective protein 3) and Pals1 (protein associated with Lin 7), assemble as apical complexes that play essential roles in regulating self-renewal and cell fate (Margolis and Borg, 2005). The unequal distribution of apical surface components during mitosis is a key determinant of daughter cell fate in *C. elegans* and *Drosophila* (Fishell and Kriegstein, 2003; Kemphues, 2000; Siller and Doe, 2009; Wodarz, 2005). Recently, mammalian Par3 was shown to promote asymmetric cell division by specifying differential Notch signaling in radial glial daughter cells (Bultje et al., 2009), suggesting that the inheritance of the apical complex guides progenitor responses to proliferative signals as well.

Secreted signals can act at a distance to guide decisions governing progenitor proliferation and cell fate (Johansson et al., 2010), but little is known of how secreted signals interact with cell-autonomous ones. Insulin-like growth factor 1 (Igf1) promotes progenitor proliferation (Hodge et al., 2004; Popken et al., 2004). Insulin/Igf1 signaling is regulated by E-catenin in keratinocytes (Vasioukhin et al., 2001) and β-catenin in oligodendrocyte progenitors (Ye et al., 2010), suggesting that cell polarity proteins govern cellular responses to extrinsic cues.

Direct interactions between Par3 and Pten (phosphatase and tensin homolog) (Feng et al., 2008; Pinal et al., 2006; von Stein et al., 2005; Wu et al., 2007) suggest that the apical complex interacts with growth factor signaling pathways. Indeed, disrupting the apical complex via *Pals1* leads to attenuated pS6 signaling, premature cell cycle exit, and rapid cell death, resulting in the absence of nearly the entire cerebral cortex (Kim et al., 2010). In turn, *Pals1*-deficiency can be partially rescued by concomitant activation of mTOR (mammalian target of rapamycin) (Kim et al., 2010), a downstream effector of growth factor signaling. Growth factor signaling, in particular via the type 1 Igf receptor (Igf1R), mediates powerful, age-dependent effects on the development and maintenance of many organ systems

including the brain through the regulation of progenitor cell division (Baker et al., 1993; Hodge et al., 2004; Liu et al., 2009; Popken et al., 2004; Randhawa and Cohen, 2005). Nevertheless, the mechanisms coordinating the availability of Igf ligands to cortical progenitor cells have remained unclear.

Though vascular sources of secreted proliferative signals are well characterized (Palmer et al., 2000; Shen et al., 2004, 2008; Tavazoie et al., 2008), the apical surfaces of early cortical precursors and their primary cilia do not approximate blood vessels but instead directly contact the cerebrospinal fluid (CSF) (Fuchs and Schwark, 2004; Kim et al., 2010), suggesting that secreted factors may interact with progenitor cells at this interface. The CSF proteome shows a complex and dynamic pattern of protein expression (Dziegielewska et al., 1981; Parada et al., 2005; Zappaterra et al., 2007), suggesting important roles beyond provision of a fluid cushion for the central nervous system and maintenance of extracellular ionic balance. The CSF has recently been implicated in carrying secreted proteins in several contexts, including Fgf2 to midbrain progenitors (Martín et al., 2006), Sonic hedgehog to cerebellar progenitors (Huang et al., 2010) and Slit guidance of neuroblasts in adult brain (Sawamoto et al., 2006). Regulation of cerebral cortical progenitor cells by growth factors distributed in the lateral ventricular CSF would provide potentially global control over cerebral cortical neurogenesis, but this hypothesis has not been examined.

Here, we show that the apical complex couples autonomous regulation of progenitor proliferation to CSF-borne signals in the developing cerebral cortex. *Pals1* and *Pten* interact genetically to regulate cerebral cortical size and progenitor proliferation and have opposing roles in localizing the Igf1R to the apical domain of cortical progenitors. Apically localized Igf1Rs respond to CSF-borne Igf ligands, particularly Igf2, and CSF regulates cortical progenitor proliferation in an Igf2-dependent fashion. Finally, CSF Igf2 concentration is elevated in patients with malignant glioblastoma, suggesting that CSF proteins may regulate CNS tumorigenesis. Our findings suggest that the apical complex couples autonomous and extrinsic signaling in cerebral cortical progenitors, enabling these cells to respond appropriately to diffusible CSF-borne signals that regulate cortical neural stem cells during development and disease.

RESULTS

Genetic Interactions of *Pals1* and *Pten* at the Apical Surface Region

Since *Pals1* loss disrupts growth factor signaling and cortical development (Kim et al., 2010), we looked for potential interactions of *Pals1* with other regulators of growth factor signaling and found genetic interactions between *Pals1* and *Pten* (Groszer et al., 2001). Cerebral cortex-specific deletion of *Pals1* was achieved by crossing mice with a conditional *Pals1* allele ($Pals1^{loxP/loxP}$) (Kim et al., 2010) with mice carrying Emx1-promoter-driven Cre recombinase ($Emx1Cre^{+/-}$) (Gorski et al., 2002). $Pals1^{loxP/loxP}/Emx1Cre^{+/-}$ mice lacked nearly the entire cortical structure due to premature cell cycle exit and cell death (Kim et al., 2010), with heterozygotes having an intermediate phenotype (Figure 1A). In contrast, *Pten* deficiency, obtained by crossing $Pten^{loxP/loxP}$ mice (Groszer et al., 2001) with either $Emx1Cre^{+/-}$ or $NestinCre^{+/-}$ mice, resulted in cortical hyperplasia arising from excessive and extended proliferation of apical progenitors (Figure 1A; see Figures S1A–S1E available online; Groszer et al., 2001). While the broadest groupings of cells were preserved in *Pten* mutants, the cortical plate was disorganized across its entire radial extent (Figures S1A–S1C). No phenotypic abnormalities were observed in either heterozygous $Pten^{loxP/+}/NestinCre^{+/-}$ mice or in $Pten^{loxP/loxP}/NestinCre^{-/-}$ littermate controls (Figure S1A and data not shown). Conditional deletion of *Pten* in the $Pals1^{loxP/+}/Emx1Cre^{+/-}$ mice resulted in an almost normal cortical size (Figure 1A). Histological analyses of $Pals1^{loxP/+}/Emx1Cre^{+/-}$ mice or $Pten^{loxP/+}/Pals1^{loxP/+}/Emx1Cre^{+/-}$ mice revealed a severely disrupted laminar organization of the dorsomedial cortex (Figure 1B; Kim et al., 2010). Double mutants showed a relatively normal organization of the marginal zone (Figure 1B), consistent with a genetic interaction between the apical complex and *Pten*. The expression of apical complex components, especially Cdc42, were abnormal in *Pten* cortex (Figure S1F and data not shown). The proportion of proliferative progenitor cells marked by Ki67-positive staining cells was greater in the double mutant cortex compared to conditional *Pals1* heterozygotes (Figure 1C) and brain size was also more normal by embryonic day (E) 14.5 (Figures S1G and S1H). Proportions of early-born neurons marked by Tbr1 and Ctip2 were also more normal in the $Pten^{loxP/loxP}/Pals1^{loxP/+}/Emx1Cre^{+/-}$ mice than in either *Pals1* or *Pten* mutants alone (Figure 1D and data not shown). However, cells in the double mutant brain appeared irregular in size and lamination (Figure 1D), a finding consistent with roles for *Pten* in the regulation of cell size and polarity (Figure S1C; Chalhoub et al., 2009; Groszer et al., 2001) and with a role for *Pten* downstream of the apical complex.

The genetic interaction between *Pals1* and *Pten* and the decreased proliferation of progenitors and prominent cell death in *Pals1* mutants (Kim et al., 2010) prompted us to test whether the apical complex interacts with Igf signaling, since Igfs play a prominent role in cell cycle kinetics of cortical progenitors, cell survival, and brain size (Hodge et al., 2004; Liu et al., 2009; Popken et al., 2004; Schubert et al., 2003). The Igf1R, which binds both Igf1 and Igf2, mediates the proliferative response to Igf signaling (Weber et al., 1992). Surprisingly, Igf1R was enriched in cortical progenitors at the apical, ventricular surface, interdigitating with β-catenin (Figures 2A–2D), suggesting the apical region as the likely site for binding of Igf1R ligand. Apical Igf1R expression was strikingly decreased in $Pals1^{loxP/loxP}/Emx1Cre^{+/-}$ mice (Figure 2E). By contrast in the absence of *Pten*, Igf1R immunoreactivity demonstrated a considerable basolateral spread in clusters of radial glia (Figure 2F and data not shown). Analyses of downstream signaling events, using a specific antibody against the phosphorylated form of Rsk substrate S6 ribosomal protein (phospho-S6rp), revealed an apical pattern of activity within control brains (Figure 2G). In contrast in *Pten* mutants, phospho-S6rp showed a broad distribution across the cortical tissue, with many robust phospho-S6rp-positive cells extending basally away from the lateral ventricle (Figure 2G). While the majority of cells positive for Igf1R were clearly apical progenitors, some upregulation of Igf1R in basal progenitors is possible. Though we cannot rule

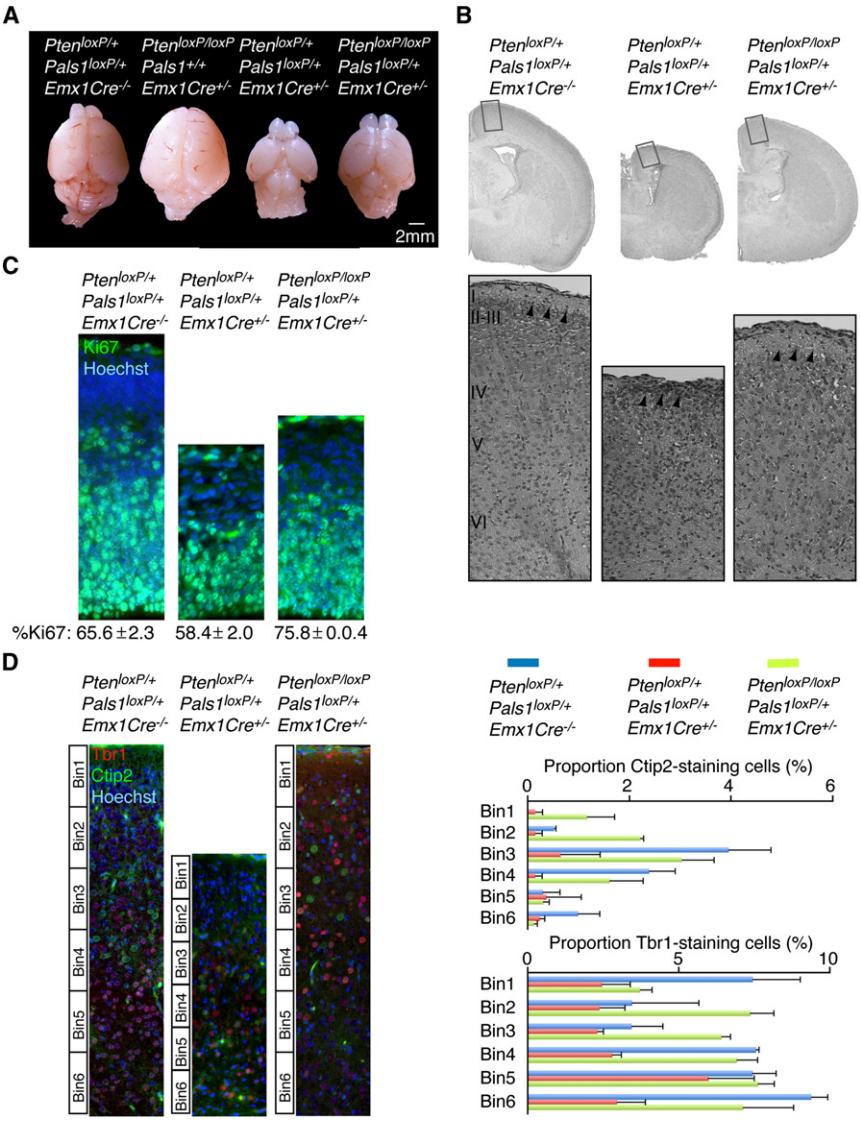

Figure 1. The Apical Complex and *Pten* Modulate Brain Size

(A) Conditional *Pten* deletion (*Pten*$^{loxP/loxP}$/*Pals1*$^{+/+}$*Emx1Cre*$^{+/-}$) resulted in hyperplasia and an enlarged cerebral cortex. Ablation of *Pten* in *Pten*$^{loxP/loxP}$/*Pals1*$^{loxP/+}$/*Emx1Cre*$^{+/-}$ mice largely restored the small brain phenotype of *Pten*$^{loxP/+}$/*Pals1*$^{loxP/+}$/*Emx1Cre*$^{+/-}$ neonates.

(B) H&E staining of *Pten*$^{loxP/+}$/*Pals1*$^{loxP/+}$/*Emx1Cre*$^{-/-}$, *Pten*$^{loxP/+}$/*Pals1*$^{loxP/+}$/*Emx1Cre*$^{+/-}$, and *Pten*$^{loxP/loxP}$/*Pals1*$^{loxP/+}$/*Emx1Cre*$^{+/-}$ neonates. Arrowheads point to marginal zone.

(C) The proportion of Ki67-positive staining progenitors was restored in the E14.5 *Pten*$^{loxP/loxP}$/*Pals1*$^{loxP/+}$/*Emx1Cre*$^{+/-}$ cortex compared to *Pten*$^{loxP/+}$/*Pals1*$^{loxP/+}$/*Emx1Cre*$^{+/-}$ (percent Ki67-positive staining cells ± SEM; *Pten*$^{loxP/+}$/*Pals1*$^{loxP/+}$/*Emx1Cre*$^{-/-}$, 65.6 ± 2.3; *Pten*$^{loxP/+}$/*Pals1*$^{loxP/+}$/*Emx1Cre*$^{+/-}$, 58.4 ± 2.0; *Pten*$^{loxP/loxP}$/*Pals1*$^{loxP/+}$/*Emx1Cre*$^{+/-}$, 75.8 ± 0.4; ANOVA, $p < 0.01$, $n = 3$).

(D) Left panels: representative images of Ctip2-positive and Tbr1-positive staining neurons analyzed in *Pten*$^{loxP/+}$/*Pals1*$^{loxP/+}$/*Emx1Cre*$^{-/-}$, *Pten*$^{loxP/+}$/*Pals1*$^{loxP/+}$/*Emx1Cre*$^{+/-}$, and *Pten*$^{loxP/loxP}$/*Pals1*$^{loxP/+}$/*Emx1Cre*$^{+/-}$ neonates. Right panels: the cortical plate was subdivided into six equal bins and Ctip2 and Tbr1 positive cells quantified per bin are expressed as percent of total cells per bin. *Pten* deletion in the *Pten*$^{loxP/loxP}$/*Pals1*$^{loxP/+}$/*Emx1Cre*$^{+/-}$ mice restored the proportions of early-born cells marked by Tbr1 and Ctip2 (percent positive staining cells/total: *Pten*$^{loxP/+}$/*Pals1*$^{loxP/+}$/*Emx1Cre*$^{-/-}$ Ctip2 = 8.13 ± 2.0, Tbr1 = 38.7 ± 2.4; *Pten*$^{loxP/+}$/*Pals1*$^{loxP/+}$/*Emx1Cre*$^{+/-}$ Ctip2 = 1.6 ± 1.2, Tbr1 = 18.8 ± 3.1; *Pten*$^{loxP/loxP}$/*Pals1*$^{loxP/+}$/*Emx1Cre*$^{+/-}$ Ctip2 = 8.5 ± 1.6, Tbr1 = 39.1 ± 2.6; ANOVA, $p < 0.05$, $n = 3$).

See also Figure S1.

out that *Pals1* and *Pten* could function independently to regulate Igf signaling and cortical growth, we interpret our data to suggest that within the cortical ventricular zone, *Pals1* and *Pten* spatially restrict IgfR expression and Igf signaling to the apical membrane domain.

Loss and gain of Igf signaling in mutant mice produced phenotypes similar to those seen when apical complex signaling is disrupted. Mice with Igf1R deficiency limited to neural precursors (*Igf1R*$^{loxP/loxP}$/*NestinCre*$^{+/-}$) were microcephalic (Figure 2H–2J; Kappeler et al., 2008; Liu et al., 2009) and had a reduced frequency of phospho-Histone H3 (PH3, a marker of cell division) proliferative progenitors in the ventricular zone (PH3-positive cells/100 μm VZ ± SEM at E16.5: control, 2.9 ± 0.3; *Igf1R*$^{loxP/loxP}$/*NestinCre*$^{+/-}$, 1.7 ± 0.1; unpaired t test, $p < 0.01$; $n = 4$ and $n = 3$, respectively). We did not observe differences in progenitor cell survival at the ventricular zone in these mice as assessed by cleaved caspase 3 (CC3) immunoreactivity (data not shown). Conversely, mice with increased Igf activity (Igf1 expressed from the human *GFAP* promoter) were macrocephalic (data not shown) (Ye et al., 2004) and had increased proliferative progenitors at the ventricular surface (PH3-positive cells/100 μm VZ ± SEM at E18.5: control, 0.9 ± 0.08; *Igf1_Tg*, 1.2 ± 0.07; unpaired t test, $p < 0.05$, $n = 3$ and $n = 4$, respectively). Together with published work demonstrating that *Insulin receptor substrate 2* (*Irs2*) deletion leads to microcephaly (Schubert et al., 2003), these data suggest that Igf signaling in cortical progenitors, facilitated at the apical surface via Pals1 and an intact apical complex, regulates cortical development.

CSF-Borne Igf Signaling

The normal apical localization of the Igf1R, and the fact that we did not observe *Igf1* or *Igf2* mRNA in neural progenitor cells by in situ hybridization (Figures 3A, 3B, and data not shown; Ayer-le Lievre et al., 1991), suggested that progenitor cells may be exposed to Igfs derived from the lateral ventricle CSF. We confirmed the presence of Igf2 in an unbiased tandem mass

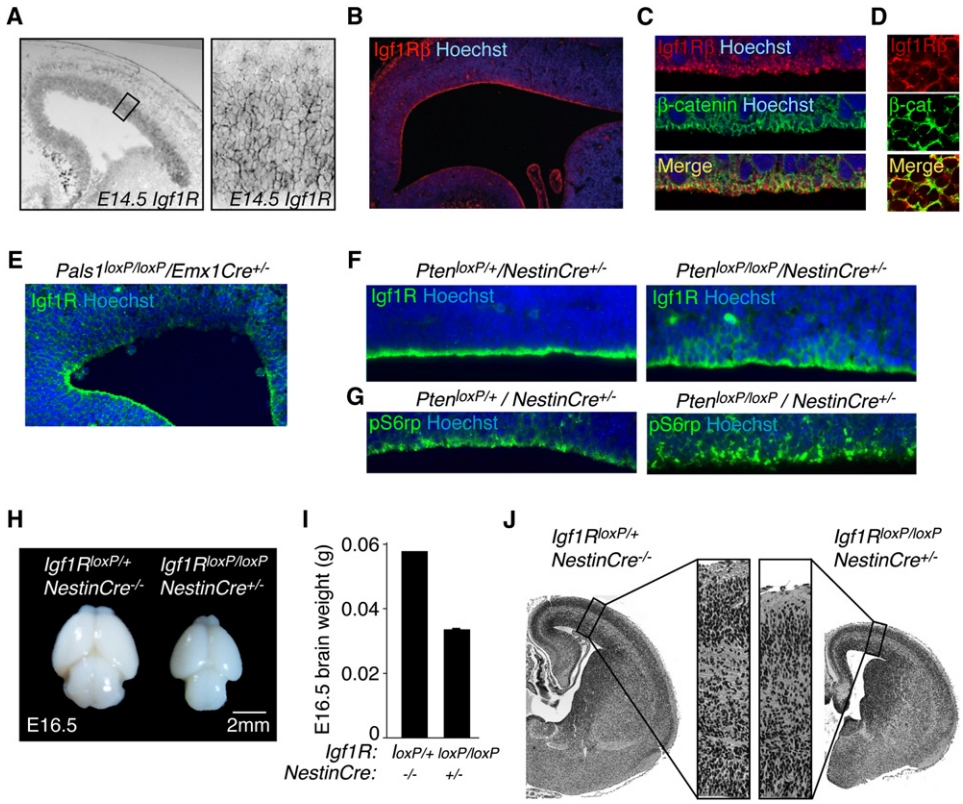

Figure 2. Igf1R Expression in Cortical Progenitor Cells

(A) Left panel: *Igf1R* in situ hybridization at E14.5 mouse. Right panel: high-magnification image of area denoted in left panel.

(B) Igf1R enriched along the ventricular surface of E17 rat cortex.

(C) Confocal images of Igf1Rβ and β-catenin immunostaining in rat E17 ventricular zone.

(D) En face view of the mouse E16.5 ventricular zone immunostained with Igf1Rβ and β-catenin.

(E) Ventricular Igf1R expression was disrupted in E12.5 $Pals1^{loxP/loxP}/Emx1Cre^{+/-}$ cortex.

(F) Left panel: Igf1R expression was enriched along the apical, ventricular zone of E14.5 $Pten^{loxP/+}/NestinCre^{+/-}$ controls. Right panel: Igf1R expression expanded basolaterally in $Pten^{loxP/loxP}/NestinCre^{+/-}$ radial glia.

(G) Left panel: pS6rp activity along the ventricular progenitors of E14.5 $Pten^{loxP/+}/NestinCre^{+/-}$ controls. Right panel: pS6rp localization extended basolaterally in $Pten^{loxP/loxP}/NestinCre^{+/-}$ radial glia. See also Figure S1.

(H) *Igf1R* deficiency in NestinCre expressing cells diminished brain size at E16.5.

(I) Brain weights of $Igf1R^{loxP/loxP}/NestinCre^{+/-}$ and controls at E16.5 (brain weight (g) ± SEM: $Igf1R^{loxP/loxP}/NestinCre^{+/-}$: 0.06; $Igf1R^{loxP/loxP}/NestinCre^{+/-}$: 0.03 ± 0.001; n = 2 [+/+], n = 3 [−/−]).

(J) H&E staining of brains shown in (H).

spectrometry (LC-MS/MS) analysis of CSF (Table S1; Binoux et al., 1986) and detected Igf1 in CSF by ELISA (E14 CSF [Igf1], 72.2 ng/ml, n = 2; E17 CSF [Igf1], 69.6 ng/ml; adult CSF [Igf1], 68.8 ng/ml, n = 3). Igf1 expression in the CSF remained stable across the ages sampled (see above). In contrast, expression of Igf2 in rat CSF was temporally dynamic; it peaked during periods of neurogenesis and declined in adulthood (Figure 3C). High levels of *Igf2* mRNA expression by the choroid plexus suggested this as a source of CSF Igf2 (Figure 3B), and quantitative PCR revealed that rat choroid plexus expressed 10.7-fold more Igf2 than its cortical counterpart at E17 (data not shown). We confirmed that Igf2 mRNA was also expressed in vascular endothelial cells, and leptomeninges in the rat embryo at E14 and E17 as well as pericytes at E17 (Figures 3A, 3B, and data not shown; Bondy et al., 1992; Dugas et al., 2008; Stylianopoulou et al., 1988), suggesting that extrachoroidal sources of Igf2 may contribute to CSF-Igf2 content as well. Immunogold labeling revealed Igf2 binding to progenitors along the apical, ventricular surface (Figure 3D). Moreover, Igf2 binding to progenitors was highly enriched along primary cilia (Figure 3E), which extend directly into the ventricular space (Figure 3F; Cohen et al., 1988). We did not observe enriched Igf2 binding beyond the apical surface of ventricular zone progenitor cells (data not shown). Thus, the robust expression of Igf2 by the choroid plexus and the apical binding of Igf2 to progenitors along the ventricular zone strongly suggest that the CSF distributes choroid plexus secreted Igf2 to cortical progenitor cells.

Purified rat E17 CSF directly stimulated Igf1R mediated signaling activity, reflected by Igf1Rβ phosphorylation as well as phosphorylation of Akt and MAPK (Figure 3G), two downstream targets of Igf signaling as well as other growth factors that may be present in CSF. Igf2 treatment by itself induced Igf

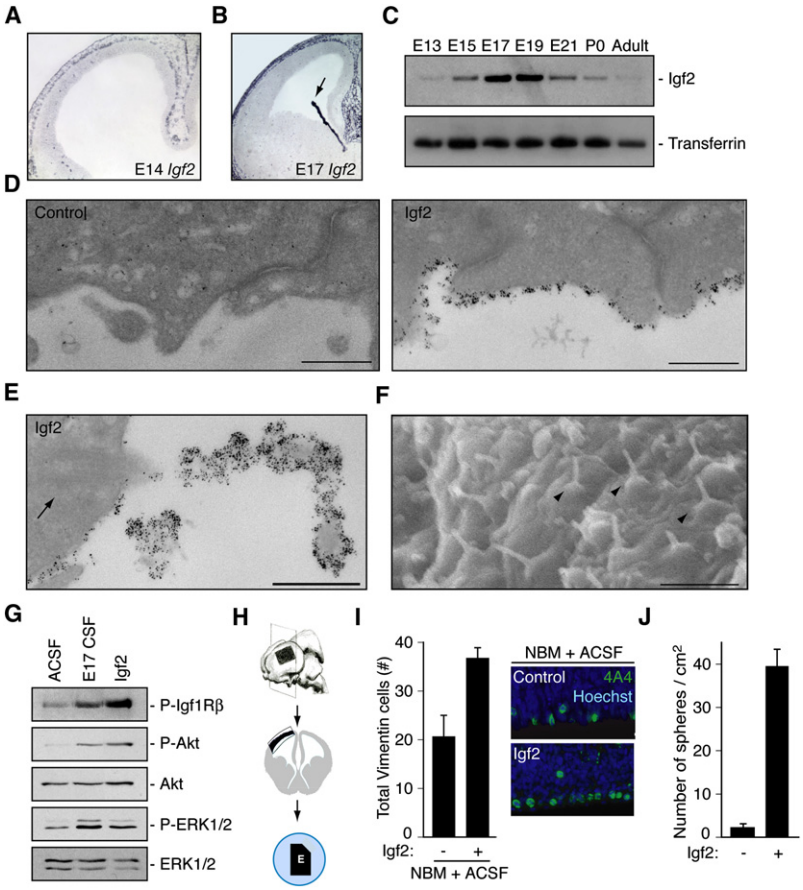

Figure 3. Igf2 Is Expressed in Cerebrospinal Fluid and Stimulates Progenitor Proliferation

(A and B) *Igf2* in situ hybridization of rat E14 and E17 cortex. Arrow points to choroid plexus.

(C) Transient Igf2 expression in rat CSF.

(D) Immunogold labeling of endogenous Igf2 in E17 rat brain. Left panel: no primary control. Right panel: Igf2 binding to ventricular surface of cortical progenitors. Scale bar represents 500 nm.

(E) Igf2 binding to primary cilium of cortical progenitor cell. Arrow points to ciliary basal body. Scale bar represents 500 nm.

(F) Scanning EM of mouse ventricular surface at E12.5. Arrowheads point to primary cilia projecting into the ventricular space. Scale bar represents 2 μm.

(G) Lysates of cortical cells deprived of growth factors for 6 hr and treated with ACSF, E17 CSF, or Igf2 for 5 min were immunoblotted with antibodies to P-Igf1R, P-Akt, Akt, P-ERK1/2, and ERK1/2.

(H) Schematic of cortical explant dissections: explant placed on membrane with ventricular side down contacting CSF and notch making medial-caudal side.

(I) Left panel: E16 explants cultured with NBM plus 20% ACSF (control) or with supplemental Igf2 immunostained with anti-Vimentin 4A4 and Hoechst represented as mean ± SEM (Igf2 mean, 36.7 ± 2.1; control mean, 20.4 ± 4.46; n = 8; Mann-Whitney; $p < 0.005$). Vimentin 4A4-positive cells increased in explants cultured with Igf2 compared to control. Right panels: representative images of explants quantified in left panels.

(J) Single cells dissociated from primary neurospheres cultured in control media or control media containing Igf2 (20 ng/ml). Igf2 stimulated secondary sphere formation after 10 DIV (Igf2 mean, 39.3 ± 4.1; control mean, 2.2 ± 0.75; n = 3; t test; $p < 0.005$).

See also Table S1.

signaling similar to embryonic CSF (Figure 3G). Igf2 binding to progenitors, the localization of the Igf1R, its phosphorylation, as well as the phosphorylation of its downstream targets Akt and MAPK in response to CSF, strongly suggest that the CSF is a primary source of Igf ligands for cerebral cortical neuroepithelial cells, although additional sources cannot be completely excluded.

We next tested whether Igf2 supports progenitor proliferation in a cerebral cortical explant system. In this system, rat embryonic cortex dissected from the lateral pallium is placed on polycarbonate membranes and floated on defined media (Figure 3H). We found that Igf2 added to neurobasal medium (NBM) with 20% artificial CSF (ACSF) stimulated the proliferation of progenitor cells marked by phospho-Vimentin 4A4 in rat cortical explants (Figure 3I; Noctor et al., 2002). In addition, Igf2 treatment alone maintained GLAST-positive neurospheres, an in vitro model of neural stem cells, even in the absence of Fgf2 (fibroblast growth factor 2) and Egf (epidermal growth factor) (Figure 3J; Vescovi et al., 1993). Finally, pharmacologic activation of the signaling pathway with insulin demonstrated that activation of Igf signaling by ligands other than Igf2 is sufficient to stimulate proliferation (PH3-positive cells/100 μm VZ ± SEM in E16 rat explant: control mean, 5.6 ± 0.7; insulin (10 μg/ml) mean, 11.2 ± 0.4; Mann-Whitney, $p < 0.05$; n = 6). Therefore, Igf signaling modulates proliferation of isolated cortical precursors or those maintained in their pallial environment in vitro.

CSF Promotes Proliferation of Progenitor Cells in an Age-Dependent Manner

Since the CSF is a complex fluid containing many factors including Igf binding proteins that may modulate Igf2 bioavailability and signaling (Figures 4A and 4B; Table S1; Clemmons, 1997; Zappaterra et al., 2007), we tested whether native CSF alone could support cortical tissue growth. We used a heterochronic "mix-and-match" approach for exposing cortical tissue to CSF collected at different ages. E16 rat cortical explants with intact meninges and vasculature cultured with 100% E17 rat CSF for 24 hr, without any additional exogenous media or factors, retained remarkable tissue architecture, cell viability, and proliferation, approximating in vivo E17 rat cortex (Figure 4C). In contrast, E16 explants cultured with 100% artificial CSF failed to thrive, had decreased mitotic activity, disorganized neuronal morphology, and increased cell death (Figures 4C, S2A, and S2B). Filtration analysis of E17 CSF showed that the sizes of CSF factors that support stem cells likely range from 10 kDa–100 kDa, suggesting that they are proteins (Table S2 and data not shown). Thus, the embryonic CSF proteome provides essential growth and survival factors for the developing cortex.

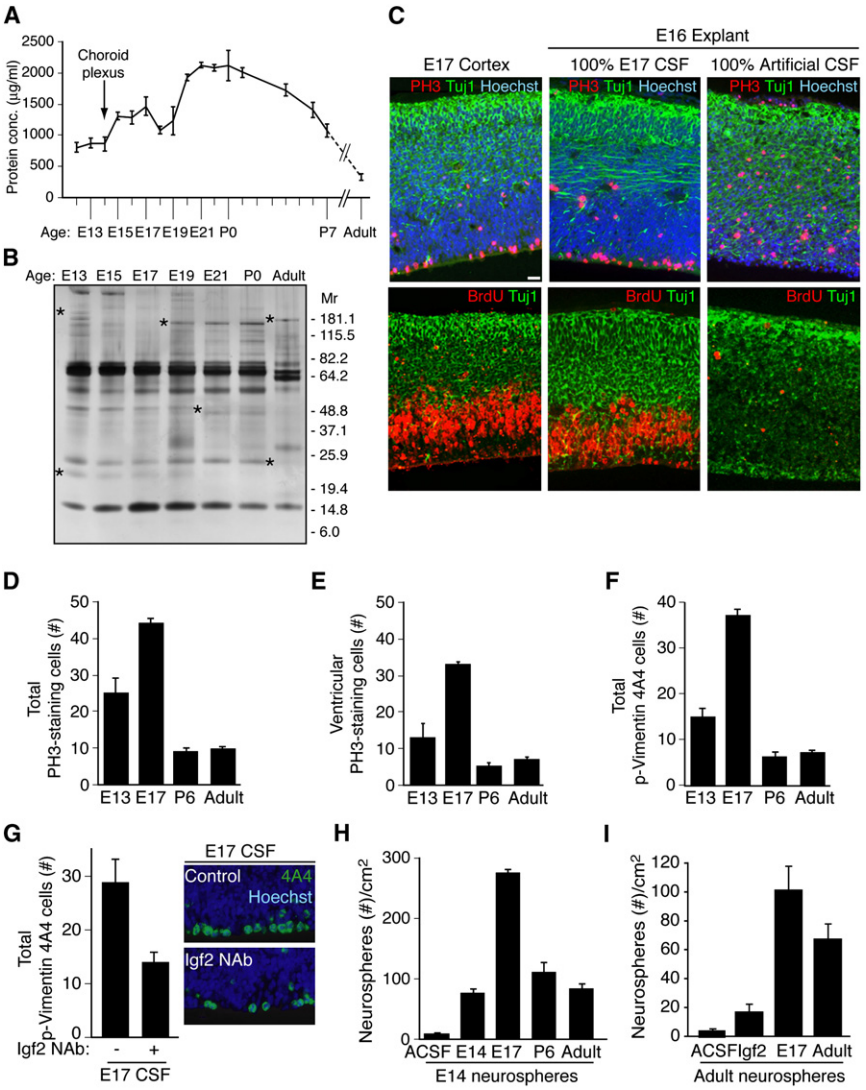

Figure 4. Embryonic CSF Supports Cortical Explant Viability and Stimulates Proliferation of Neural Progenitor Cells

(A) Total CSF protein concentration over the course of rat development.

(B) Silver stain of embryonic rat CSF revealed a dynamic fluid with numerous changes in protein composition over time. Asterisks indicate proteins with varying CSF expression during development.

(C) E17 rat cortex and E16 explants grown for 24 hr in 100% embryonic E17 CSF or 100% artificial CSF, respectively. Upper panels: anti-PH3 (red), and anti-Tuj1 (green), Hoechst (blue) immunostaining. Lower panels: anti-BrdU (red) and anti-Tuj1 (green) immunostaining. Explants cultured in 100% E17 CSF in vitro maintained tissue histology similar to embryo in vivo. Survival and proliferation of explants cultured with E17 CSF indicated by immunoreactivity for PH3 along the ventricular surface, BrdU incorporation in the ventricular zone, and Tuj1-positive-staining neurons in the developing cortical plate.

(D) E16 explants cultured in 100% E13, E17, P6, or adult CSF for 24 hr were immunostained with anti-PH3 (see Figure S2C). Quantification of total PH3-positive-staining cells per 400 μm explant showed that proliferating cells increased in explants cultured with E17 CSF compared to E13, P6, or adult CSF. Immuno-positive cells are represented as mean ± SEM (E17 mean, 44.1 ± 1.43; E13 mean, 25 ± 4.2; P6 mean, 9.2 ± 0.8; adult mean, 9.6 ± 0.9, n = 4; Kruskal-Wallis; $p < 0.005$).

(E) Quantification of ventricular PH3-staining cells in explants (D). PH3-positive cells along the ventricle were significantly increased in explants cultured with E17 CSF compared to E13, P6, or adult CSF (E17 mean, 32.3 ± 0.79; E13 mean, 12.8 ± 3.9; P6 mean, 4.9 ± 1.0; adult mean, 6.9 ± 0.73; n = 4; Kruskal-Wallis; $p < 0.01$).

(F) E16 explants (D) immunostained with anti-Vimentin 4A4 (see Figure S2C) were quantified. Vimentin 4A4-positive cells were significantly increased in explants cultured with E17 CSF compared to E13, P6, or adult CSF (E17 mean, 37.1 ± 1.4; E13 mean, 14.9 ± 1.9; P6 mean, 6.1 ± 1.05; adult mean, 7.3 ± 0.6; n = 4; Kruskal-Wallis; $p < 0.005$).

(G) Left panel: E16 explants cultured in control E17 CSF or E17 CSF with Igf2 neutralizing antibody (Igf2 NAb), immunostained with anti-Vimentin 4A4 and Hoechst (E17 control mean, 28.8 ± 4.3; E17 IGF2 NAb mean, 13.9 ± 2.0; n = 4; Mann-Whitney; $p < 0.05$). Vimentin 4A4-positive cells decreased in explants cultured with E17 CSF plus Igf2 NAb compared to control. Right panels: representative images of explants quantified in left panels.

(H) Primary neurospheres derived from E14 cortex were grown in 20% artificial (A), E14, E17, P6, or adult CSF for 10 days in vitro (DIV). E17 CSF generated the most spheres/cm^2 (E17 mean, 274 ± 8.0; E14 mean, 77 ± 7.0; P6 mean, 110 ± 17.5; adult mean, 81 ± 8.8; n = 3; ANOVA; $p < 0.005$). See also Figure S2.

(I) Neurospheres derived from adult rat SVZ were cultured in artificial (A)CSF, Igf2 (20 ng/ml), E17 CSF, or adult rat CSF for 10DIV. Igf2, E17 CSF, and adult CSF supported the growth and maintenance of adult neurospheres (ACSF, 4.76 ± 0.67; Igf2, 17.3 ± 3.2; E17 CSF, 101.7 ± 15.8; adult CSF, 67.8 ± 12.6; Kruskal-Wallis, Igf2 versus E17 CSF, $p < 0.05$; E17 CSF versus adult CSF, N.S.; n = 3).

See also Figure S2 and Tables S2 and S3.

By comparing rat CSF from several ages, we determined that the effects of CSF on survival and proliferation are strikingly age dependent and mimicked the temporal profile of CSF-Igf2 expression (Figure 3C). E17 CSF (near the middle of neurogenesis) maintained the healthiest explants and produced the maximal increase in the frequency of PH3-labeled proliferating cells in E16 cortical explants compared to explants cultured with E13 (early in neurogenesis), P6, or adult CSF (Figures 4D, 4E, S2C, and data not shown). Many mitotic cells were identified as proliferating neuroepithelial progenitor cells by their immunoreactivity for phospho-Vimentin (4A4; Figures 4F and S2C). In contrast, no differences were seen in Tbr2-positive basal progenitors, which do not contact the CSF directly (data not shown). Together, these data suggest that age-dependent differences in CSF signals are both supportive and instructive for neuroepithelial precursor proliferation in the developing cortex. The CSF effects may be specific to neuroepithelial progenitors, which contact the ventricle through the apical

complex, without affecting the intermediate progenitors of the SVZ.

We tested directly whether CSF-borne Igf2 was necessary to explain the effects of age-specific CSF on rat cortical explants. The frequency of proliferating cells declined in explants grown in E17 CSF in the presence of Igf2 neutralizing antibodies (Igf2 Nab; Figure 4G). Igf2 neutralization with Igf2 NAb did not interfere with Igf1 levels in CSF compared to control as assayed by ELISA (data not shown). While Igf signaling is known to promote neuronal survival (Popken et al., 2004), we did not observe differences in ventricular progenitor cell survival in these explant experiments (data not shown), suggesting that Igf actions on neural cell survival likely depends on the cell type, developmental stage, and microenvironment. These data confirm the important role for CSF borne Igf2 in regulating cerebral cortical progenitor cells but do not rule out roles of other CSF borne factors as well.

CSF Influence on Isolated Neural Stem Cells Requires Igf Signaling

Neural stem cells cultured as neurospheres confirmed the age-dependent capacity of CSF to maintain neural stem cells (Reynolds and Weiss, 1996) and provided additional evidence suggesting that Igf2-mediated signaling is an essential determinant of CSF activity on neural stem cells. CSF from any age supported the proliferation and maintenance of isolated cortical stem cells cultured as primary or secondary neurospheres (Figure 4H and data not shown; Vescovi et al., 1993). However, E17 CSF was maximally effective in generating increased numbers of neurospheres, larger neurospheres, and maintained neurospheres even in long-term cultures for up to 44 days in vitro (Figures 4H, S2D–S2G, and data not shown). Neurospheres grown in CSF retained responsiveness to Fgf2 and Egf, indicating that the CSF maintains stem cells in an uncommitted fate (Figure S2H). CSF generated neurospheres from adult SVZ precursors as well (Figure 4I). Consistent with these observations and our explant studies, the Igf1R inhibitor picropodophyllin blocked the formation of spheres in the presence of E17 CSF (data not shown). Our data suggest that the choroid plexus is the most prominent source of Igf2 in CSF (Figures 3 and S3A). Accordingly, media conditioned with E17 choroid plexus provided enhanced support for neurosphere formation compared to media conditioned with embryonic cortex, adult choroid plexus, or adult brain (Table S3), demonstrating that one or more factors actively secreted from the embryonic choroid plexus, including potentially Igf2, is sufficient for stem cell growth and maintenance. Thus, distinct factors secreted by the choroid plexus into the embryonic CSF, including Igf2, confer E17 CSF with an age-associated advantage to stimulate and maintain neural stem cell proliferation, and Igf signaling is likely one pathway that promotes this process.

Genetic Inactivation of Igf Signaling Impairs Brain Development

Mouse explant experiments confirmed a requirement for Igf signaling in the proliferation of progenitor cells. Mouse embryonic CSF supported the survival and proliferation of mouse cortical progenitors (C57BL/6 explants: 20% ACSF in NBM mean, 7.4 ± 0.2; 20% E16.5 CSF in NBM mean, 14.1 ± 1.4; Mann-Whitney; $p < 0.01$; $n = 3$), and purified Igf2 in 20% ACSF in NBM stimulated cortical progenitor proliferation (Figure 5A). When the *Igf1R* was genetically inactivated in cortical progenitors (*Igf1R*$^{loxP/loxP}$/*NestinCre*$^{+/-}$) (Liu et al., 2009), wild-type CSF no longer stimulated cortical progenitor proliferation (ACSF, 17.6 ± 2.9; E16.5 CSF, 16.4 ± 3.0; Mann-Whitney; N.S.; $n = 3$). Importantly, CSF obtained from *Igf2*$^{-/-}$ mice failed to stimulate progenitor proliferation in wild-type explants compared to control (Figure 5B), suggesting that Igf2 in its native CSF environment stimulates proliferation of progenitor cells during cerebral cortical development.

As expected for the roles we have shown for Igf2 in regulating proliferation, we found that *Igf2*-deficiency reduced brain size (Figure 5C). *Igf2*$^{-/-}$ brain weight decreased by 24% at P8 compared to controls (Figure 5D). Accordingly, the overall cortical perimeter and surface area were reduced in *Igf2*$^{-/-}$ brains compared to controls as well (Figures 5E–5G). Profound defects in somatic size couple to brain size (Purves, 1988). As previously reported (DeChiara et al., 1991; Baker et al., 1993), *Igf2*$^{-/-}$ body weight was reduced compared to control (mean body weight (g) at P8: *Igf2*$^{+/+}$, 5.6 ± 0.01; *Igf2*$^{-/-}$, 2.8 ± 0.1; Mann-Whitney; $p < 0.0001$; $n = 11$), suggesting that Igf2 may be a secreted factor that scales brain size to body size. Consistent with the mouse CSF Igf2 expression pattern that is significantly increased during later embryonic development (Figure S3B), blunting Igf2 expression markedly reduced the proliferating progenitor cells at E16.5 compared to controls (PH3-positive cells/100 μm VZ ± SEM at E16.5: *Igf2*$^{+/+}$, 2.5 ± 0.3; *Igf2*$^{-/-}$, 1.7 ± 0.1; Mann-Whitney; $p < 0.05$; $n = 5$). NeuN- and late-born Cux1-staining neurons were reduced in *Igf2*$^{-/-}$ mice (Figure 5H and data not shown), confirming that Igf2 contributes to cortical progenitor proliferation and to late stages of neurogenesis. Taken together, our genetic experiments support a model in which the apical complex localizes Igf signaling in progenitors by ensuring the apical, ventricular localization of the Igf1R. In this manner, the apical complex couples cell autonomous and extracellular signals to the regulation of cortical development.

Glioblastoma CSF Expresses High Igf2

Our data, together with recent findings implicating Igf signaling in the maintenance of adult neural stem cells (Llorens-Martín et al., 2010), raised the possibility that abnormalities of the CSF may be relevant to conditions showing abnormal proliferation, including in glioblastoma multiforme (GBM), a malignant astrocytic brain tumor. Igf-PI3K-Akt signaling has been implicated as a key regulator of gliomagenesis (Louis, 2006; Soroceanu et al., 2007), and mutations in *PTEN* are commonly found in patients with GBM (Louis, 2006). We analyzed Igf2 concentration in a panel of 56 human GBM patient CSF samples collected from 21 individuals representing the full range of disease progression and 8 disease-free controls and found that CSF from GBM patients contained significantly more Igf2 than CSF from disease-free controls (Igf2 concentration expressed as mean ± SEM for GBM patients, 340.4 ± 12.9 ng/ml; $n = 56$; disease-free controls, 222.9 ± 41.5 ng/ml; $n = 8$; Mann-Whitney, $p < 0.01$). Three GBM samples containing the highest Igf2 concentrations (605.8 ng/ml,

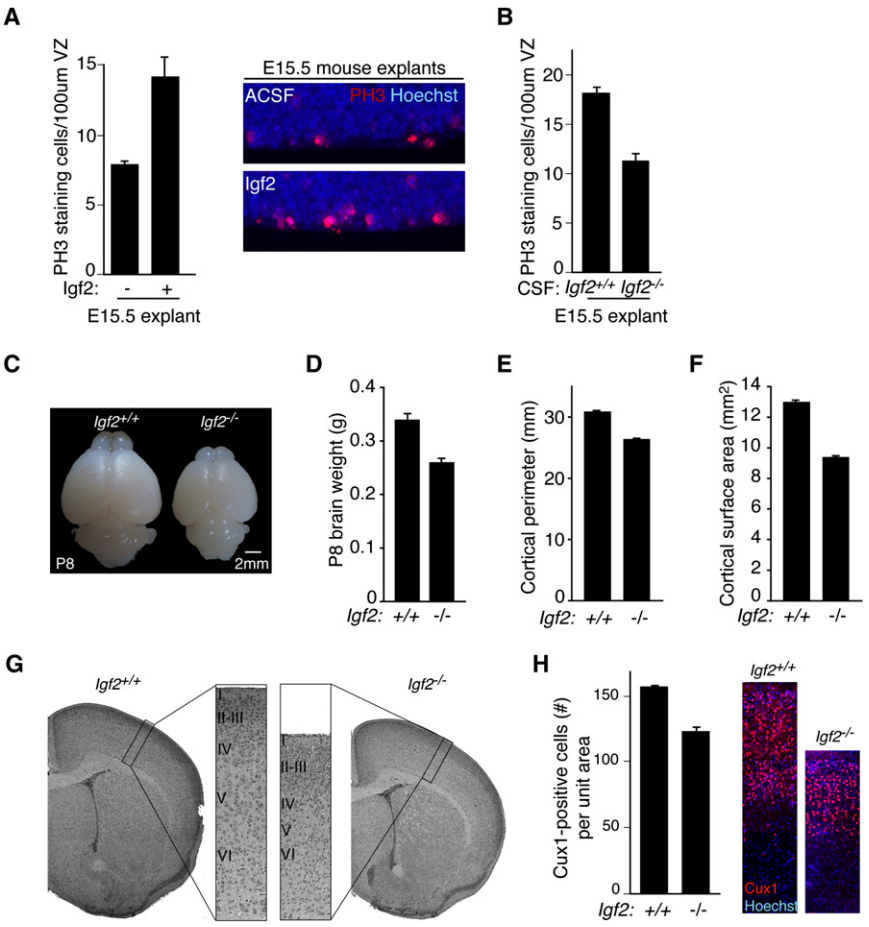

Figure 5. CSF Igf2 Regulates Progenitor Proliferation and Brain Size

(A) Left panels: E15.5 C57BL/6 explants cultured in NBM supplemented with 20% ACSF or ACSF/Igf2. Igf2 stimulated the proliferation of PH3-positive cortical progenitor cells (C57BL/6 explants: ACSF mean, 7.4 ± 0.2; Igf2 mean, 11.2 ± 0.3; Mann-Whitney, $p < 0.05$; $n = 3$). Right panels: representative images of explants quantified in left panels.

(B) E15.5 C57BL/6 explants cultured in NBM supplemented with 20% E16.5 wild-type or *Igf2*$^{-/-}$ CSF. *Igf2*-deficient CSF failed to stimulate progenitor cell proliferation compared to control (*Igf2*$^{+/+}$,17.9 ± 0.8; *Igf2*$^{-/-}$ CSF, 11.4 ± 1.0; Mann-Whitney; $p < 0.06$; $n = 3$ and $n = 4$, respectively).

(C) Representative images of P8 *Igf2*$^{-/-}$ and control brains.

(D) *Igf2* deficiency reduced P8 brain weight (*Igf2*$^{+/+}$, 0.34 g ± 0.008; *Igf2*$^{-/-}$, 0.26 g ± 0.004; Mann-Whitney, $p < 0.0001$, $n = 11$).

(E) *Igf2* deficiency reduced P8 cortical perimeter (*Igf2*$^{+/+}$, 30.9 mm ± 0.01; *Igf2*$^{-/-}$, 26.4 mm ± 0.1; Mann-Whitney, $p < 0.0001$, $n = 11$).

(F) *Igf2* deficiency reduced P8 cortical surface area (*Igf2*$^{+/+}$, 13.0mm^2 ± 0.1; *Igf2*$^{-/-}$, 9.4 mm^2 ± 0.1; Mann-Whitney, $p < 0.0001$, $n = 11$).

(G) H&E staining of *Igf2*$^{-/-}$ and control brains at P8.

(H) Left panels: *Igf2*$^{-/-}$ brains have reduced numbers of upper layer neurons marked by Cux1 (total Cux1-positive staining cells in equally sized cortical columns expressed as mean ± SEM: *Igf2*$^{+/+}$, 157 ± 1.5; *Igf2*$^{-/-}$, 131.3 ± 3.3; t test, $p < 0.005$, $n = 3$). Right panels: representative images of *Igf2*$^{-/-}$ and control brains quantified in left panels.

See also Figure S3.

502.8 ng/ml, and 468.7ng/ml) came from patients with advanced disease (Figure 6A and Table 1). By contrast, the three patients with the lowest levels of Igf2 (142.1 ng/ml, 145.4 ng/ml, and 153.9 ng/ml) all had early or stable glioma (Figure 6A and Table 1). Similar to rodent ventricular CSF, human lumbar CSF stimulated cortical progenitor cell proliferation in our explant assay, with CSF from GBM patients causing greater proliferation than CSF from disease-free controls (Figure 6B). Moreover, human GBM patient CSF neutralized with Igf2 antibodies failed to stimulate the proliferation of progenitor cells (Figure 6B; Igf2 concentration following NAb absorption, GBM1(PBS): 605.8 ng/ml; GBM1 (NAb), 45.6 ng/ml; GBM2(PBS), 502.8 ng/ml; GBM2(NAb), 218.3 ng/ml; GBM3(PBS), 468.7 ng/ml; GBM3(NAb), 248.8 ng/ml). Taken together, these data suggest that beyond embryonic brain development, CSF-Igf2, in particular, is a potential mediator of GBM pathology and that the CSF mechanisms that normally regulate neural stem cells are misregulated in GBM.

CSF-Mediated Long-Range Distribution of Additional Secreted Factors

Whereas our studies suggest an important role for Igf2 in controlling proliferation in late stages of neurogenesis and potentially postnatally, they do not rule out the presence of other secreted factors that may act at long ranges via the CSF, and so we performed functional screening tests for several other families of factors. The CSF contained Wnt signaling activity (Zhou et al., 2006), based upon phosphorylation of LRP6, a Wnt coreceptor in response to CSF exposure (Figure 7A). Several Wnt ligands were expressed along the ventricular surface and in the choroid plexus (Figure 7B and data not shown; Grove et al., 1998). Frizzled (Fz) receptors, which bind LRP6 to transduce Wnt signals, showed enhanced expression in ventricular progenitors (Figure 7B and data not shown; Zhou et al., 2006), suggesting that CSF may distribute Wnts to precursors throughout the ventricular surface. Additional signaling activities that influence cortical development were also found in the CSF, with responsive cells seen broadly in the ventricular zone. There were dynamic levels of bone morphogenetic protein (Bmp) activity in the CSF during different stages of cortical development (Figure 7C). Using a luciferase-based assay in which overall Bmp activity can be quantified between 0.1 and 100 ng/ml (data not shown), we found that Bmp activity in the CSF decreased during embryogenesis and peaked in adulthood (Figure 7C). CSF-borne Bmp activity may be responsible for stimulating progenitors widely throughout the cortical ventricular zone in vivo, based on

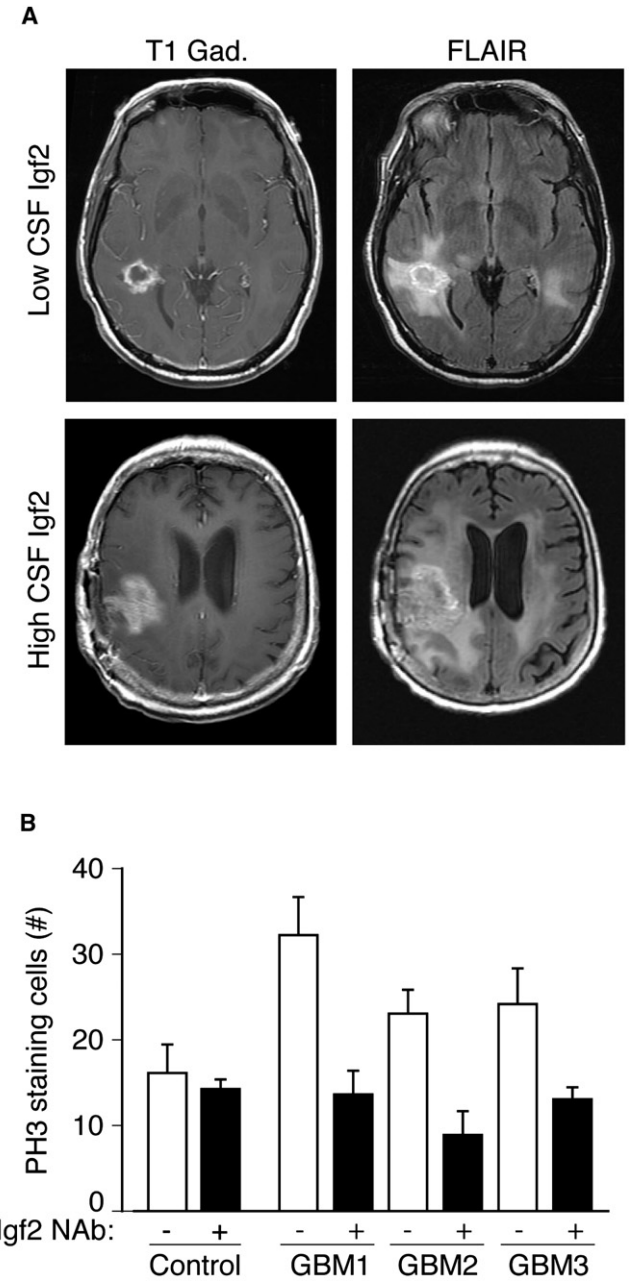

Figure 6. Glioblastoma CSF Igf2 Supports Progenitor Proliferation

(A) MRI scans from subjects with low and high CSF Igf2 levels. Gadolinium-enhanced T1-weighted (T1-Gad) MRI sequence delineated the contrast-enhanced portion of the tumor where tumor angiogenesis developed. Fluid attenuation inversion recovery (FLAIR) images included area of nonvascularized and invasive tumor (Macdonald et al., 1990).

(B) Twenty percent human GBM CSF in NBM stimulated PH3-positive proliferating cells compared to an average of three disease-free control CSFs in E16 rat explants (control = 16.0 ± 4.1 [n = 3]; GBM1 = 32.3 ± 4.3 [n = 4]; GBM2 = 23.0 ± 2.8 [n = 5]; GBM3 = 23.4 ± 3.8 [n = 4]; Mann-Whitney, $p < 0.05$). Igf2(NAb) inhibited GBM CSF-stimulated progenitor proliferation (GBM1 = 13.5 ± 2.9 [n = 4]; GBM2 = 9.0 ± 2.7 [n = 4]; GBM3 = 13.0 ± 1.5 [n = 3]; Mann-Whitney, $p < 0.05$). CSF Igf2 concentration before and after Igf2 NAb absorption: GBM1(PBS) = 605.8 ng/ml; GBM1(NAb) = 45.6 ng/ml; GBM2(PBS) = 502.8 ng/ml; GBM2(NAb) = 218.3 ng/ml; BM3(PBS) = 468.7 ng/ml; GBM3(NAb) = 248.8 ng/ml).

widespread labeling for nuclear phospho-SMAD1/5/8 (Figure 7D) in the absence of any known Bmp ligands localizing to the ventricular zone (Shimogori et al., 2004), whereas Bmps 2, 4, 5, and 7 are expressed in embryonic and adult choroid plexus (Figure 7E; Hébert et al., 2002; Shimogori et al., 2004). Moreover, growth and differentiation factors 3 and 8 (GDF3 and GDF8), both members of the TGF-β superfamily of proteins that can influence Bmp signaling (Levine and Brivanlou, 2006) were found in our MS analyses of CSF (data not shown), though we do not consider our MS analysis to have recovered all potential smaller ligands in the CSF. Retinoic acid (RA) (Haskell and LaMantia, 2005; Siegenthaler et al., 2009) activity in CSF also varied over the course of cortical development (Figure 7F). A luciferase-based assay that quantifies RA activity ranging between 10^{-9} and 10^{-6}M (data not shown) revealed that RA activity in CSF peaked early and decreased in adulthood (Figure 7F). In parallel, RA responsive cortical progenitors localized to the developing ventricular zone (Figure 7G). Similar to Wnts and Bmps, RA is most likely released into CSF since RA synthetic and catabolic enzymes were expressed in the choroid plexus (Figure 7H) and meninges (data not shown). Thus, CSF shows bioavailability of a wide range of activities known to regulate neurogenesis, patterning, and neuronal survival in the cerebral cortex and throughout the CNS.

DISCUSSION

We show that the CSF plays an essential, active role in distributing signals in the central nervous system. The key findings of our study are (1) the apical complex is essential for the apical localization of Igf1R; (2) *Pten* deficiency in the *Pals1* background results in an almost normally sized brain; (3) CSF Igf2 binds to the apical domain of cortical progenitor cells, stimulating their proliferation in an age-dependent manner; (4) Igf2 is upregulated in GBM patient CSF, contributing to the range of proliferative activities of GBM patient CSF; and (5) the CSF provides an adaptive library of secreted factors throughout life. The dynamic regulation of several potent modulators of neural stem cells reinforces the central relationship between local signaling at the apical surface via ligands delivered by the CSF during cortical neurogenesis.

Asymmetric Growth Factor-Based Signaling

It has been suggested that asymmetry of signaling at the apical versus basolateral aspect of cortical progenitors regulates progenitor progress through the cell cycle (Bultje et al., 2009; Sun et al., 2005). The basolateral expansion of the Igf1R signaling domain we report in *Pten* mutants suggests potential links between asymmetric growth factor signaling and proliferation. Although asymmetric localization of the EgfR in cortical progenitors has previously been reported (Sun et al., 2005), the ventricular enrichment of the Igf1R was not known and raises the possibility that the apical enrichment of the Igf1R along with other apical proteins confers a differential responsiveness to mitogenic signals, akin to Notch signaling (Bultje et al., 2009). Since Igfs are potent mitogens for cortical progenitors (Hodge et al., 2004; Popken et al., 2004), one model might suggest that inheritance of the apical complex promotes progenitor fate by differentially concentrating Igf1R and its

Table 1. Clinical Presentation of GBM Patients with Lowest and Highest CSF Igf2 Concentrations

			Clinical Presentation		
	Patient	[Igf2] ng/ml	Tumor size: T1-Gad (cm^2)	Tumor size: FLAIR (cm^2)	Life Span
Low CSF Igf2	L1	142.1	7.14	6.46	Stable disease at follow-up; 3 weeks post-CSF collection
	L2	145.4	8.50	54.12	Stable disease at follow-up; 3 weeks post-CSF collection
	L3	153.9	5.94	20.5	Stable disease at follow-up; 5 weeks post-CSF collection
High CSF Igf2	H1	605.8	47.31	102.83	Deceased at 1 week post-CSF collection
	H2	502.8	13.69	53.90	Deceased at 52 weeks post-CSF collection
	H3	468.7	23.94	36.48	Deceased at 30 weeks post-CSF collection

Patients with the lowest CSF Igf2 concentrations (L1–L3) had early or stable GBM disease state, while patients with the highest CSF Igf2 concentrations (H1–H3) had advanced disease and aggressive tumor progression at time of CSF collection. Tumor size was determined by Macdonald's criteria, where T1-Gad MRI sequence delineated the contrast-enhanced portion of tumor, and FLAIR images include areas of nonvascularized and invasive tumor (Macdonald et al., 1990). High-CSF Igf2 patients had larger T1-Gad tumor sizes compared to low-CSF Igf2 patients (Mann-Whitney; $p < 0.05$; n=3).

downstream signaling proteins into cells that retain their perikarya or at least a process (likely a cilium) in the ventricular zone, causing these cells to remain in the cycling pool. The presence of proliferation-inducing factors in the CSF suggests that withdrawal of the progenitor's apical ventricular process may be an important step in neuronal differentiation (Cappello et al., 2006), by insulating progenitor cells from proliferative signals in CSF, with vascular niches potentially supplying sources of secreted factors for stem cells at other stages (Palmer et al., 2000; Shen et al., 2004, 2008; Tavazoie et al., 2008).

Our data provides a new perspective on the production and provision of Igf ligands, which are known to regulate stem cell populations in the brain and other proliferative epithelia (Bendall et al., 2007; Hodge et al., 2004; Liu et al., 2009; Popken et al., 2004; Ye et al., 2004; Zhang and Lodish, 2004). In the E17 rat brain, the choroid plexus was the strongest source of Igf2, though we cannot discount a contribution by the vasculature or other cellular sources of Igf2 that may percolate into the CSF. Indeed, both pericytes and endothelial cells express Igf2 (Dugas et al., 2008), and Igfs from vascular tissue may have local effects beyond apically mediated Igf1R signaling shown here. Thus, locally derived Igf2 may play distinct roles at different developmental time points and in different cellular contexts, and Igf signaling may also be influenced by CSF Igf1 and insulin. Although Igf2 availability decreased in adult CSF (Figures 3C and S3B), *Igf2* continued to be expressed in adult choroid plexus (data not shown) and maintained adult neurospheres (Figure 4I), suggesting that low levels of CSF Igf2 contribute to the maintenance of adult neural stem cells. The aberrant increase in Igf2 in advanced GBM patients reinforces the hypothesis that Igf signaling has an influence on proliferation of cortical precursors. Our identification of *Igf2* regulation of neurogenesis and brain size complements a literature in which Igf signaling is well known to influence body and brain size (Baker et al., 1993; DeChiara et al., 1991; Purves, 1988), raising the intriguing possibility that Igf2 represents a secreted factor that may scale brain size to body size.

Fluid-Based Signaling in the CNS and Beyond

The activity of growth promoting factors in the CSF and their action on progenitors across the apical surface may be a model for other epithelia including lung, gut, and vascular endothelia that develop in relation to extracellular fluids (Bendall et al., 2007; Scadden, 2006). Extracellular fluid apparently regulates the microenvironment of hematopoietic stem cells, where Igf signaling regulates progenitor proliferation (Orkin and Zon, 2008; Zhang and Lodish, 2004). The differential capacity of Igf signaling to confer a proliferative advantage to stem cells may be regulated in part by Igf's interactions with binding proteins or other secreted factors in the environment (Clemmons, 1997). Our experiments focused on the age-associated effects of CSF on survival and proliferation across the cortical ventricular zone. However, the distribution of CSF resident proteins, as well as the flow of the CSF, may also influence ciliary orientation and maturing ependymal cell polarity (Mirzadeh et al., 2010), which create activity gradients as has been shown for Slit (Sawamoto et al., 2006).

If a major component of the stem cell niche reflects secreted factors acting at long distances from their sources, modulation of the proteomic composition of extracellular fluids may also provide unexpected ways to regulate stem cell behavior in health and disease. For example, while Igf2 activity peaked in embryonic CSF, some CSF-borne Igf persisted in adulthood (Figures 3, S3B, and data not shown). Igf2 and Igf1 in adult CSF may contribute to the retention of neural stem cell properties in the adult SVZ (Doetsch et al., 1999). Importantly, the regulation of CSF growth factors may also extend to pathologic states. Igf2 and other diffusible growth factors that drive neural progenitor proliferation during development are upregulated in some GBM patients (Louis, 2006; Soroceanu et al., 2007), and GBM patients have elevated Igf2 levels in their CSF. CSF $A\beta_{1-42}$ and phosphorylated Tau levels were recently shown to assist in Alzheimer's disease diagnosis (De Meyer et al., 2010). Thus, modulation of the proteomic composition of extracellular fluids together with the integration of cell autonomous determinants of self-renewal by the apical complex may ultimately provide unexpected ways to regulate stem cell behavior in health and disease.

EXPERIMENTAL PROCEDURES

Animals

Time pregnant Sprague-Dawley, C57BL/6, and Swiss Webster dams were purchased from Charles River Laboratories and Taconic. *Pals1*$^{loxP/loxP}$/*NestinCre*$^{+/-}$, *Pals1*$^{loxP/loxP}$/*Emx1Cre*$^{+/-}$, *Igf1R*$^{loxP/loxP}$/*NestinCre*$^{+/-}$, and

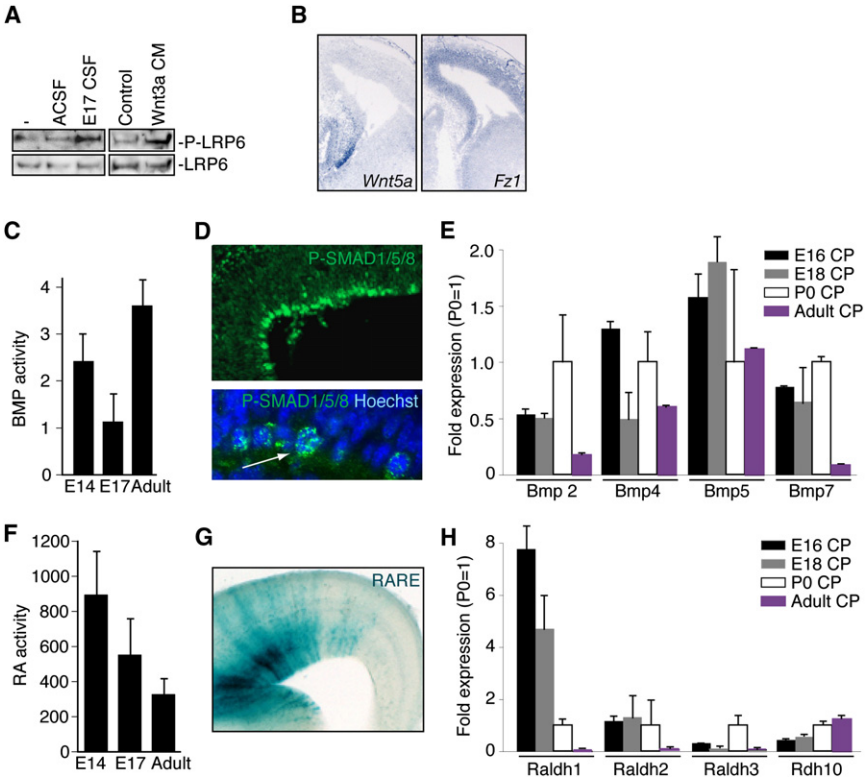

Figure 7. The CSF Proteome Coordinates Multiple Signaling Pathways that Regulate Brain Development

(A) Lysates of cortical cells were left untreated or treated with 20% ACSF or E17 CSF and 10% Wnt3a conditioned medium or its control medium for 2 hr and subjected to immunoblotting with the P-LRP6 or LRP6 antibodies.

(B) In situ hybridization for *Wnt5a* and *Fz1* in mouse E14.5 cortex.

(C) Bmp activity was measured in E14, E17, and adult rat CSF as luciferase signal in a clonally derived Bmp-sensitive cell line. Responses were compared to linear responses generated in the same cell line by pure ligand (Bmp4; data not shown). Bmp activity levels varied with age and were statistically significant between E17 and adult (ANOVA, $p < 0.001$; $n = 4$).

(D) Top panel: expression and nuclear localization of phospho-Smad (P-SMAD) 1/5/8 in E14 rat cortical ventricular cells. Bottom panel: arrow points to expression and nuclear localization of P-SMAD1/5/8 in E16.5 mouse cortical ventricular cells.

(E) qPCR measurement of Bmps 2, 4, 5, and 7 in the E16, E18, P0, and adult rat choroid plexus (CP).

(F) Quantification of RA activity in E14, E17, and adult rat CSF. RA activity declined, based on comparison of CSF activation of an RA responsive, clonally derived cell line with response to RA at known concentrations, from midgestation through adulthood (ANOVA, $p = 0.07$; $n = 4$).

(G) RA responsive progenitor cells at the cortical ventricular zone from an E16.5 DR5-RARE transgenic mouse (LaMantia et al., 1993).

(H) qPCR of Raldh1, 2, 3, and Rdh10, in rat CP.

GFAP:Igf_1Tg mice were obtained from heterozygous breedings, and *Pten*$^{loxP/+}$/*Pals1*$^{loxP/+}$/*Emx1Cre*$^{+/-}$, and *Pten*$^{loxP/loxP}$/*Pals1*$^{loxP/+}$/*Emx1Cre*$^{+/-}$ mice were obtained from *Pten*$^{loxP/+}$/*Pals1*$^{loxP/loxP}$/*Emx1Cre*$^{+/-}$ and *Pten*$^{loxP/loxP}$/*Emx1Cre*$^{-/-}$ crosses (Groszer et al., 2001; Kim et al., 2010; Liu et al., 2009; Ye et al., 2004). *Igf2*$^{-/-}$ and control CSF was collected from embryos obtained from homozygous breedings. *Igf2*$^{-/-}$ and control P8 brains were obtained from homozygous crosses or paternal heterozygotes mated with homozygous knockouts (DeChiara et al., 1991). All animal experimentation was carried out under protocols approved by the IACUCs of Harvard Medical School, Children's Hospital Boston, and UNC-Chapel Hill.

Antibodies

The following antibodies were purchased: Ctip2, Igf2 (for EM), Tbr2 (Abcam); BrdU (AbD Serotec); Ki67 (Abnova); Vimentin 4A4 (Assay Designs); Pax6 (Developmental Studies Hybridoma Bank); β-catenin, Cdc42 (BD Biosciences); AKT, phospho-AKT, Igf1R, phospho-Igf1R, CC3, and phospho-S6rp (Cell Signaling); GLAST (Chemicon); Tuj1 (Covance); HRP conjugated anti-Transferrin (Immunology Consultants Laboratory, Inc.); Igf2 (NAb; Millipore); Cux1, Igf2 (for WB) (Santa Cruz Biotechnology); and phospho-Histone H3 (Upstate). Tbr1 was a kind gift of R. Hevner.

CSF Isolation

Embryonic rodent CSF, isolated as described (Zappaterra et al., 2007), was kept on ice during collection, centrifuged at 10,000 × g at 4°C for 10 min., and stored at −80°C. Human GBM and disease-free CSF samples were collected by lumbar puncture from patients undergoing clinical evaluation. The 56 GBM samples tested were obtained from 21 individuals representing the full-range of disease progression. The samples used in analyses of highest and lowest CSF Igf2 concentration were obtained from distinct individuals. All research was approved by the IRBs at BIDMC and Children's Hospital Boston.

Cortical Explants

The telencephalic wall was dissected onto polycarbonate membranes (Whatman; 13 mm, 8.0 μm) and cultured for 24 hr as described in text. Artificial (A)CSF (NaCl 119 mM, KCl 2.5 mM, $NaHCO_3$ 26 mM, NaH_2PO_4 1 mM, glucose 11 mM, $MgCl_2$ 2 mM, $CaCl_2$ 2.8 mM) was supplemented with Igf2 (2 ng/ml; US Biologicals) as indicated. Igf2 NAb antibody was incubated with E17 CSF for 1 hr at 4°C. Explants were pulsed with BrdU for 30 min and fixed (60% methanol, 30% chloroform, and 10% acetic acid; 10 min). For in vivo BrdU labeling, pregnant dams were administered a 3 hr BrdU (60 mg/kg) pulse. Tissue was paraffin sectioned (5 μm).

SUPPLEMENTAL INFORMATION

Supplemental Information includes three figures, three tables, and Supplemental Experimental Procedures and can be found with this article online at doi:10.1016/j.neuron.2011.01.023.

ACKNOWLEDGMENTS

We thank A. Bonni, S. Gygi, R. Segal, and members of the Walsh laboratory for helpful discussions; H. Steen for assistance with mass spectrometry; D. Rubin and J. Sheng for pMSCVhyg-Igf2; U. Berger, J. Buchanan, M. Ericsson, Y. Lin, A. Peters, C. Kourkoulis, and S. White for technical assistance. This work was supported by a Sigrid Jusélius Fellowship, an Ellison/AFAR Postdoctoral Fellowship, and Award Number K99NS072192 from the NINDS (M.K.L); a Stuart H.Q. & Victoria Quan Fellowship (M.W.Z.), a NIH MSTP grant (M.W.Z. and Y.J.Y.); the Child Neurology Foundation (X.C.); *A Reason To Ride* research fund (M.L. and E.T.W.), a NINDS grant (RO1 NS048868) (A.J.D. and P.Y.), a NICHD grant (RO1 HD008299) (A.J.D.), a NIH grant

(HD029178), and an UNC-CH Reynolds Faculty Fellowship (A.S.L.); a NINDS grant (3 RO1 NS032457), the Manton Center for Orphan Disease Research, and the Intellectual and Developmental Disabilities Research Centers (CHB DDRC, P30 HD18655)(C.A.W.). C.A.W. is an Investigator of the Howard Hughes Medical Institute. The content is solely the responsibility of the authors and does not necessarily represent the official views of the NINDS or the NIH.

Accepted: December 7, 2010
Published: March 9, 2011

REFERENCES

Ayer-le Lievre, C., Ståhlbom, P.A., and Sara, V.R. (1991). Expression of IGF-I and -II mRNA in the brain and craniofacial region of the rat fetus. Development *111*, 105–115.

Baker, J., Liu, J.P., Robertson, E.J., and Efstratiadis, A. (1993). Role of insulin-like growth factors in embryonic and postnatal growth. Cell *75*, 73–82.

Bendall, S.C., Stewart, M.H., Menendez, P., George, D., Vijayaragavan, K., Werbowetski-Ogilvie, T., Ramos-Mejia, V., Rouleau, A., Yang, J., Bossé, M., et al. (2007). IGF and FGF cooperatively establish the regulatory stem cell niche of pluripotent human cells in vitro. Nature *448*, 1015–1021.

Binoux, M., Lassarre, C., and Gourmelen, M. (1986). Specific assay for insulin-like growth factor (IGF) II using the IGF binding proteins extracted from human cerebrospinal fluid. J. Clin. Endocrinol. Metab. *63*, 1151–1155.

Bondy, C., Werner, H., Roberts, C.T., Jr., and LeRoith, D. (1992). Cellular pattern of type-I insulin-like growth factor receptor gene expression during maturation of the rat brain: Comparison with insulin-like growth factors I and II. Neuroscience *46*, 909–923.

Bultje, R.S., Castaneda-Castellanos, D.R., Jan, L.Y., Jan, Y.N., Kriegstein, A.R., and Shi, S.H. (2009). Mammalian Par3 regulates progenitor cell asymmetric division via notch signaling in the developing neocortex. Neuron *63*, 189–202.

Cappello, S., Attardo, A., Wu, X., Iwasato, T., Itohara, S., Wilsch-Bräuninger, M., Eilken, H.M., Rieger, M.A., Schroeder, T.T., Huttner, W.B., et al. (2006). The Rho-GTPase cdc42 regulates neural progenitor fate at the apical surface. Nat. Neurosci. *9*, 1099–1107.

Chalhoub, N., Zhu, G., Zhu, X., and Baker, S.J. (2009). Cell type specificity of PI3K signaling in Pdk1- and Pten-deficient brains. Genes Dev. *23*, 1619–1624.

Clemmons, D.R. (1997). Insulin-like growth factor binding proteins and their role in controlling IGF actions. Cytokine Growth Factor Rev. *8*, 45–62.

Cohen, E., Binet, S., and Meininger, V. (1988). Ciliogenesis and centriole formation in the mouse embryonic nervous system. An ultrastructural analysis. Biol. Cell *62*, 165–169.

DeChiara, T.M., Robertson, E.J., and Efstratiadis, A. (1991). Parental imprinting of the mouse insulin-like growth factor II gene. Cell *64*, 849–859.

De Meyer, G., Shapiro, F., Vanderstichele, H., Vanmechelen, E., Engelborghs, S., De Deyn, P.P., Coart, E., Hansson, O., Minthon, L., Zetterberg, H., et al; Alzheimer's Disease Neuroimaging Initiative. (2010). Diagnosis-independent Alzheimer disease biomarker signature in cognitively normal elderly people. Arch. Neurol. *67*, 949–956.

Doetsch, F., Caillé, I., Lim, D.A., García-Verdugo, J.M., and Alvarez-Buylla, A. (1999). Subventricular zone astrocytes are neural stem cells in the adult mammalian brain. Cell *97*, 703–716.

Dugas, J.C., Mandemakers, W., Rogers, M., Ibrahim, A., Daneman, R., and Barres, B.A. (2008). A novel purification method for CNS projection neurons leads to the identification of brain vascular cells as a source of trophic support for corticospinal motor neurons. J. Neurosci. *28*, 8294–8305.

Dziegielewska, K.M., Evans, C.A., Lai, P.C., Lorscheider, F.L., Malinowska, D.H., Møllgård, K., and Saunders, N.R. (1981). Proteins in cerebrospinal fluid and plasma of fetal rats during development. Dev. Biol. *83*, 193–200.

Feng, W., Wu, H., Chan, L.N., and Zhang, M. (2008). Par-3-mediated junctional localization of the lipid phosphatase PTEN is required for cell polarity establishment. J. Biol. Chem. *283*, 23440–23449.

Fishell, G., and Kriegstein, A.R. (2003). Neurons from radial glia: The consequences of asymmetric inheritance. Curr. Opin. Neurobiol. *13*, 34–41.

Fuchs, J.L., and Schwark, H.D. (2004). Neuronal primary cilia: A review. Cell Biol. Int. *28*, 111–118.

Gorski, J.A., Talley, T., Qiu, M., Puelles, L., Rubenstein, J.L., and Jones, K.R. (2002). Cortical excitatory neurons and glia, but not GABAergic neurons, are produced in the Emx1-expressing lineage. J. Neurosci. *22*, 6309–6314.

Groszer, M., Erickson, R., Scripture-Adams, D.D., Lesche, R., Trumpp, A., Zack, J.A., Kornblum, H.I., Liu, X., and Wu, H. (2001). Negative regulation of neural stem/progenitor cell proliferation by the Pten tumor suppressor gene in vivo. Science *294*, 2186–2189.

Grove, E.A., Tole, S., Limon, J., Yip, L., and Ragsdale, C.W. (1998). The hem of the embryonic cerebral cortex is defined by the expression of multiple Wnt genes and is compromised in Gli3-deficient mice. Development *125*, 2315–2325.

Haskell, G.T., and LaMantia, A.S. (2005). Retinoic acid signaling identifies a distinct precursor population in the developing and adult forebrain. J. Neurosci. *25*, 7636–7647.

Hébert, J.M., Mishina, Y., and McConnell, S.K. (2002). BMP signaling is required locally to pattern the dorsal telencephalic midline. Neuron *35*, 1029–1041.

Hodge, R.D., D'Ercole, A.J., and O'Kusky, J.R. (2004). Insulin-like growth factor-I accelerates the cell cycle by decreasing G1 phase length and increases cell cycle reentry in the embryonic cerebral cortex. J. Neurosci. *24*, 10201–10210.

Huang, X., Liu, J., Ketova, T., Fleming, J.T., Grover, V.K., Cooper, M.K., Litingtung, Y., and Chiang, C. (2010). Transventricular delivery of Sonic hedgehog is essential to cerebellar ventricular zone development. Proc. Natl. Acad. Sci. USA *107*, 8422–8427.

Johansson, P.A., Cappello, S., and Gotz, M. (2010). Stem cell niches during development - lessons from the cerebral cortex. Curr. Opin. Neurobiol. *20*, 1–8.

Kappeler, L., De Magalhaes Filho, C., Dupont, J., Leneuve, P., Cervera, P., Périn, L., Loudes, C., Blaise, A., Klein, R., Epelbaum, J., et al. (2008). Brain IGF-1 receptors control mammalian growth and lifespan through a neuroendocrine mechanism. PLoS Biol. *6*, e254. 10.1371/journal.pbio.0060254.

Kemphues, K. (2000). PARsing embryonic polarity. Cell *101*, 345–348.

Kim, S., Lehtinen, M.K., Sessa, A., Zappaterra, M.W., Cho, S.H., Gonzalez, D., Boggan, B., Austin, C.A., Wijnholds, J., Gambello, M.J., et al. (2010). The apical complex couples cell fate and cell survival to cerebral cortical development. Neuron *66*, 69–84.

LaMantia, A.S., Colbert, M.C., and Linney, E. (1993). Retinoic acid induction and regional differentiation prefigure olfactory pathway formation in the mammalian forebrain. Neuron *10*, 1035–1048.

Levine, A.J., and Brivanlou, A.H. (2006). GDF3 at the crossroads of TGF-beta signaling. Cell Cycle *5*, 1069–1073.

Liu, W., Ye, P., O'Kusky, J.R., and D'Ercole, A.J. (2009). Type 1 insulin-like growth factor receptor signaling is essential for the development of the hippocampal formation and dentate gyrus. J. Neurosci. Res. *87*, 2821–2832.

Llorens-Martín, M., Torres-Alemán, I., and Trejo, J.L. (2010). Exercise modulates insulin-like growth factor 1-dependent and -independent effects on adult hippocampal neurogenesis and behaviour. Mol. Cell. Neurosci. *44*, 109–117.

Louis, D.N. (2006). Molecular pathology of malignant gliomas. Annu. Rev. Pathol. *1*, 97–117.

Macdonald, D.R., Cascino, T.L., Schold, S.C., Jr., and Cairncross, J.G. (1990). Response criteria for phase II studies of supratentorial malignant glioma. J. Clin. Oncol. *8*, 1277–1280.

Margolis, B., and Borg, J.P. (2005). Apicobasal polarity complexes. J. Cell Sci. *118*, 5157–5159.

Martín, C., Bueno, D., Alonso, M.I., Moro, J.A., Callejo, S., Parada, C., Martín, P., Carnicero, E., and Gato, A. (2006). FGF2 plays a key role in embryonic cerebrospinal fluid trophic properties over chick embryo neuroepithelial stem cells. Dev. Biol. *297*, 402–416.

Mirzadeh, Z., Han, Y.-G., Soriano-Navarro, M., García-Verdugo, J.M., and Alvarez-Buylla, A. (2010). Cilia organize ependymal planar polarity. J. Neurosci. *30*, 2600–2610.

Noctor, S.C., Flint, A.C., Weissman, T.A., Wong, W.S., Clinton, B.K., and Kriegstein, A.R. (2002). Dividing precursor cells of the embryonic cortical ventricular zone have morphological and molecular characteristics of radial glia. J. Neurosci. *22*, 3161–3173.

Orkin, S.H., and Zon, L.I. (2008). Hematopoiesis: An evolving paradigm for stem cell biology. Cell *132*, 631–644.

Palmer, T.D., Willhoite, A.R., and Gage, F.H. (2000). Vascular niche for adult hippocampal neurogenesis. J. Comp. Neurol. *425*, 479–494.

Parada, C., Gato, A., and Bueno, D. (2005). Mammalian embryonic cerebrospinal fluid proteome has greater apolipoprotein and enzyme pattern complexity than the avian proteome. J. Proteome Res. *4*, 2420–2428.

Pinal, N., Goberdhan, D.C., Collinson, L., Fujita, Y., Cox, I.M., Wilson, C., and Pichaud, F. (2006). Regulated and polarized PtdIns(3,4,5)P3 accumulation is essential for apical membrane morphogenesis in photoreceptor epithelial cells. Curr. Biol. *16*, 140–149.

Popken, G.J., Hodge, R.D., Ye, P., Zhang, J., Ng, W., O'Kusky, J.R., and D'Ercole, A.J. (2004). In vivo effects of insulin-like growth factor-I (IGF-I) on prenatal and early postnatal development of the central nervous system. Eur. J. Neurosci. *19*, 2056–2068.

Purves, D. (1988). Body and Brain. A Trophic Theory of Neural Connections (Cambridge, MA: Harvard University Press).

Randhawa, R., and Cohen, P. (2005). The role of the insulin-like growth factor system in prenatal growth. Mol. Genet. Metab. *86*, 84–90.

Reynolds, B.A., and Weiss, S. (1996). Clonal and population analyses demonstrate that an EGF-responsive mammalian embryonic CNS precursor is a stem cell. Dev. Biol. *175*, 1–13.

Sawamoto, K., Wichterle, H., Gonzalez-Perez, O., Cholfin, J.A., Yamada, M., Spassky, N., Murcia, N.S., Garcia-Verdugo, J.M., Marin, O., Rubenstein, J.L., et al. (2006). New neurons follow the flow of cerebrospinal fluid in the adult brain. Science *311*, 629–632.

Scadden, D.T. (2006). The stem-cell niche as an entity of action. Nature *441*, 1075–1079.

Schubert, M., Brazil, D.P., Burks, D.J., Kushner, J.A., Ye, J., Flint, C.L., Farhang-Fallah, J., Dikkes, P., Warot, X.M., Rio, C., et al. (2003). Insulin receptor substrate-2 deficiency impairs brain growth and promotes tau phosphorylation. J. Neurosci. *23*, 7084–7092.

Shen, Q., Goderie, S.K., Jin, L., Karanth, N., Sun, Y., Abramova, N., Vincent, P., Pumiglia, K., and Temple, S. (2004). Endothelial cells stimulate self-renewal and expand neurogenesis of neural stem cells. Science *304*, 1338–1340.

Shen, Q., Wang, Y., Kokovay, E., Lin, G., Chuang, S.M., Goderie, S.K., Roysam, B., and Temple, S. (2008). Adult SVZ stem cells lie in a vascular niche: A quantitative analysis of niche cell-cell interactions. Cell Stem Cell *3*, 289–300.

Shimogori, T., Banuchi, V., Ng, H.Y., Strauss, J.B., and Grove, E.A. (2004). Embryonic signaling centers expressing BMP, WNT and FGF proteins interact to pattern the cerebral cortex. Development *131*, 5639–5647.

Siegenthaler, J.A., Ashique, A.M., Zarbalis, K., Patterson, K.P., Hecht, J.H., Kane, M.A., Folias, A.E., Choe, Y., May, S.R., Kume, T., et al. (2009). Retinoic acid from the meninges regulates cortical neuron generation. Cell *139*, 597–609.

Siller, K.H., and Doe, C.Q. (2009). Spindle orientation during asymmetric cell division. Nat. Cell Biol. *11*, 365–374.

Soroceanu, L., Kharbanda, S., Chen, R., Soriano, R.H., Aldape, K., Misra, A., Zha, J., Forrest, W.F., Nigro, J.M., Modrusan, Z., et al. (2007). Identification of IGF2 signaling through phosphoinositide-3-kinase regulatory subunit 3 as a growth-promoting axis in glioblastoma. Proc. Natl. Acad. Sci. USA *104*, 3466–3471.

Stylianopoulou, F., Efstratiadis, A., Herbert, J., and Pintar, J. (1988). Pattern of the insulin-like growth factor II gene expression during rat embryogenesis. Development *103*, 497–506.

Sun, Y., Goderie, S.K., and Temple, S. (2005). Asymmetric distribution of EGFR receptor during mitosis generates diverse CNS progenitor cells. Neuron *45*, 873–886.

Tavazoie, M., Van der Veken, L., Silva-Vargas, V., Louissaint, M., Colonna, L., Zaidi, B., Garcia-Verdugo, J.M., and Doetsch, F. (2008). A specialized vascular niche for adult neural stem cells. Cell Stem Cell *3*, 279–288.

Vasioukhin, V., Bauer, C., Degenstein, L., Wise, B., and Fuchs, E. (2001). Hyperproliferation and defects in epithelial polarity upon conditional ablation of alpha-catenin in skin. Cell *104*, 605–617.

Vescovi, A.L., Reynolds, B.A., Fraser, D.D., and Weiss, S. (1993). bFGF regulates the proliferative fate of unipotent (neuronal) and bipotent (neuronal/astroglial) EGF-generated CNS progenitor cells. Neuron *11*, 951–966.

von Stein, W., Ramrath, A., Grimm, A., Müller-Borg, M., and Wodarz, A. (2005). Direct association of Bazooka/PAR-3 with the lipid phosphatase PTEN reveals a link between the PAR/aPKC complex and phosphoinositide signaling. Development *132*, 1675–1686.

Weber, M.M., Melmed, S., Rosenbloom, J., Yamasaki, H., and Prager, D. (1992). Rat somatotroph insulin-like growth factor-II (IGF-II) signaling: role of the IGF-I receptor. Endocrinology *131*, 2147–2153.

Wodarz, A. (2005). Molecular control of cell polarity and asymmetric cell division in Drosophila neuroblasts. Curr. Opin. Cell Biol. *17*, 475–481.

Wu, H., Feng, W., Chen, J., Chan, L.N., Huang, S., and Zhang, M. (2007). PDZ domains of Par-3 as potential phosphoinositide signaling integrators. Mol. Cell *28*, 886–898.

Ye, P., Popken, G.J., Kemper, A., McCarthy, K., Popko, B., and D'Ercole, A.J. (2004). Astrocyte-specific overexpression of insulin-like growth factor-I promotes brain overgrowth and glial fibrillary acidic protein expression. J. Neurosci. Res. *78*, 472–484.

Ye, P., Hu, Q., Liu, H., Yan, Y., and D'Ercole, A.J. (2010). β-catenin mediates insulin-like growth factor-I actions to promote cyclin D1 mRNA expression, cell proliferation and survival in oligodendroglial cultures. Glia *58*, 1031–1041.

Zappaterra, M.D., Lisgo, S.N., Lindsay, S., Gygi, S.P., Walsh, C.A., and Ballif, B.A. (2007). A comparative proteomic analysis of human and rat embryonic cerebrospinal fluid. J. Proteome Res. *6*, 3537–3548.

Zhang, C.C., and Lodish, H.F. (2004). Insulin-like growth factor 2 expressed in a novel fetal liver cell population is a growth factor for hematopoietic stem cells. Blood *103*, 2513–2521.

Zhou, C.J., Borello, U., Rubenstein, J.L., and Pleasure, S.J. (2006). Neuronal production and precursor proliferation defects in the neocortex of mice with loss of function in the canonical Wnt signaling pathway. Neuroscience *142*, R1119–1131.